A THESIS FOR THE DEGREE OF MASTER OF SCIENCE IN FOOD AND NUTRITION

Effects of Cholesterol on Autophagy and Apoptosis in HepG2 cells

HepG2 세포주에서 콜레스테롤에 의한 자가포식과 세포 사멸 연구

August, 2016

Department of Food and Nutrition

Graduate School

Seoul National University

Sora Kim

Abstract

Effects of Cholesterol on Autophagy and Apoptosis in HepG2 cells

Sora Kim

Department of Food and Nutrition

Graduate School

Seoul National University

Background & Aims: Non-alcoholic fatty liver disease (NAFLD) is one of the most prevalent liver diseases. Recent studies have shown that cholesterol is accumulated in liver during the progression of NAFLD. Thus, increasing attention has been drawn to the role of cholesterol in the pathogenesis of the disease. Autophagy, a cellular degradative pathway, is an important self-defense mechanism to maintain cellular homeostasis in response to various stresses including lipid stimulation. In this context, this study was undertaken to determine cholesterol lipotoxicity in hepatocytes using cholesterol overloaded HepG2 cells. Precisely, whether dysregulated cholesterol homeostasis alters autophagic activity and contributes to apoptosis was investigated.

Methods: Human hepatocarcinoma cell line, HepG2 cells were treated with cholesterol with either 25 or 50 μg/mL of concentrations, which are considered to deposit cholesterol as much as the amount found in human and experimental NAFLD model. Additional treatment using 10μM chloroquine was conducted in some experiments to inhibit

lysosomal activity and degradation of autophagosome. Intracellular cholesterol level was measured by enzymatic colorimetric methods and the cell viability was determined through 3-(4,5-dimethylthiazol-2-yl)-2,5-diphenyltetrazolium bromide (MTT) assays. The relative levels of several autophagy or apoptosis related proteins were analyzed by Western blotting. Production of reactive oxygen species (ROS) was assessed by observing emission of green fluorescence following oxidation of 2′,7′-dichlorofluorescein diacetate. Lipid peroxide levels were determined by measuring cellular thiobarbituric acid reactive substances (TBARS) levels.

Results: Intracellular total cholesterol level increased in cells treated with 50 μg/mL cholesterol after 24 hours compared with vehicle treated cells. MTT assays showed dose-dependent cholesterol toxicity and microscopic observations showed reduction of cell populations compared with vehicle control cells when 25 or 50 μg/mL of cholesterol were treated. Detection of cleavage of non-erythroid spectrin and caspase-3 revealed that cholesterol treatment prominently induced the apoptosis in HepG2 cells. Meanwhile, regarding autophagy pathway, treatment of cholesterol induced the increases of LC3-II and p62 protein levels dose-dependently. Beclin-1 remained unchanged. Moreover, in a LC3-II turnover assay, cells treated with chloroquine plus cholesterol showed less LC3-II degradation than those with chloroquine alone. Cholesterol also resulted in concomitant increase of ubiquitinated protein levels. Thus, these data collectively indicated that cholesterol treatment reduced autophagic flux. To clarify whether defects in autophagy is the primary cause of cholesterol induced caspase-3 activation, cell viability was measured using MTT assay after chloroquine or/and cholesterol treatment. As a result, 10 μM chloroquine treatment induced 10.7% viability loss while 50 μg/mL cholesterol treatment 44.6% viability loss, despite similar level of autophagy inhibition. Thus, it can be inferred that blockage of autophagic flux is not enough to cause systemic

cell death, unless other toxic mechanisms are involved. Production of ROS and induction of lipid peroxides were observed after 50 μg/mL of cholesterol were treated, suggesting cholesterol accumulation induced oxidative stress. Activation of c-Jun N-terminal kinase (JNK) was also detected following the cholesterol loading. Furthermore, mitochondrial dysfunction which is strongly associated with oxidative stress was confirmed by detection of cleavage of caspase-9. Increased phosphorylation level of adenosine monophosphate-activated kinase (AMPK) was also observed, which indicates occurrence of ATP depletion.

Conclusion: These findings demonstrate that excessive hepatic cholesterol induces blockage of autophagic flux, oxidative stress and the subsequent mitochondrial dysfunction. Although reduced autophagic activity per se was insufficient to cause cholesterol induced hepatocyte apoptosis entirely, it seems to aggravate oxidative stress due to attenuated removal of dysfunctional mitochondria. Overall, the present study demonstrates that cholesterol, besides free fatty acids, may contribute to lipotoxicity occurring in the progression of NAFLD.

Keywords: Apoptosis, Autophagy, Cholesterol, HepG2 cells, Mitochondria, Oxidative stress

Student number: 2014-25275

Contents

List of Figures

List of Abbreviations

AMPK: Adenosine monophosphate-activated kinase

Atg: Autophagy related gene

ER: Endoplasmic reticulum

FC: Free cholesterol

GSH: Glutathione

H_2DCFDA: 2′,7′-dichlorodihydrofluorescein diacetate

JNK: c-Jun N-terminal kinase

LC3: Microtubule-associated protein light chain 3

NAFLD: Non-alcoholic fatty liver disase

NASH: Non-alcoholic steatohepatitis

PI3K: phosphatidylinositol 3-kinase

ROS: Reactive oxygen species

TBARS: Thiobarbituric acid reactive substances

TC: Total cholesterol

TG: Triacylglycerol

I. Introduction

1. Cholesterol-mediated lipotoxicity in NAFLD development

1.1. Cholesterol metabolism in the liver

Since hepatocytes are exposed to a great flux of cholesterol, unless cholesterol synthesis and uptake are counterbalanced by cholesterol removal, hepatic cholesterol accumulation occurs. Thus, balance among cholesterol de novo synthesis, uptake from all classes of plasma lipoprotein and efflux from hepatocytes is tightly regulated to maintain cholesterol levels within a specific range. Briefly, the synthesis of cholesterol occurs in the endoplasmic reticulum (ER) and is strictly regulated by the 3-hydroxy-3-methyl-glutaryl-CoA reductase. The uptake of cholesterol from lipoproteins occurs through surface proteins, including low density lipoprotein receptor and scavenger receptor BI. Regardless of its origin, metabolic pathways of hepatic cholesterol are either efflux into the blood in the form of VLDL-C or through ATP-binding cassette transporters A1 to nascent HDL-C particles, excretion via ATP-binding cassette transporters G5/G8, deposition as cholesteryl ester, or substrate for bile acid synthesis (Ioannou, 2016). Multiple cholesterol metabolic and transport-related genes are involved in the highly orchestrated metabolic and trafficking pathways, under regulation of Sterol regulatory element-binding protein-2, liver X receptor α and farnesoid X receptor. Furthermore, within the hepatocyte, cholesterol must be sorted and localized in different regions and organelles. Different lipid composition among organelles are kept steady, for example, plasma membrane holds nearly 60 % of the cellular sterol, while the ER accounts for only 5 % (Mesmin *et al.*, 2013). This unequal partition of sterol among organelles is important to exert normal cellular function.

1.2. Cholesterol accumulation and NAFLD

Non-alcoholic fatty liver disease (NAFLD) is considered as fat deposition in the liver exceeding 5% by weight while <10g of daily alcohol is consumed (Byrne *et al.*, 2009). The disease refers to a broad spectrum of liver disease encompassing simple steatosis, steatohepatitis, advanced fibrosis, and cirrhosis (Byrne *et al.*, 2009). Though it is widely accepted that lipotoxicity plays a central role in development of NAFLD and the progression from simple steatosis to non-alcoholic steatohepatitis (NASH), the exact lipotoxic molecules have not been agreed on. To date, studies of molecular mechanism of NAFLD have mainly focused on triacylglycerol (TG) or free fatty acids, but a growing body of evidence suggests that an increased level of hepatic cholesterol is a leading factor in the development of the disease (Caballero *et al.*, 2009; Mari *et al.*, 2006; Min *et al.*, 2012; Puri *et al.*, 2007; Simonen *et al.*, 2011; Van Rooyen *et al.*, 2011). Extensive dysregulation of hepatic cholesterol homeostasis with increases in hepatic cholesterol level in NAFLD has been documented. Previous studies, which took lipidomic approaches to quantify the major lipid classes in the livers of NAFLD patients, have shown increases in hepatic cholesterol levels (Caballero *et al.*, 2009; Puri *et al.*, 2007). When wild-type rats were fed a choline-deficient or a hypercholesterolemia diet was fed, free cholesterol (FC), but not free fatty acids or TG, turned out to be responsible of inflammatory cytokines-mediated steatohepatitis through mitochondrial glutathione (GSH) depletion (Mari *et al.*, 2006). The results were also confirmed in Niemann-Pick disease, type C1-defecient mice and obese ob/ob mice model (Mari *et al.*, 2006). In another study, foz/foz mice were fed high-fat diets with varying percentages of cholesterol and displayed an increase in hepatic FC level. Hepatic FC level cove rrelated with histologic severity of NASH, while hepatic levels of TG, diacylglycerol,

monoacylglycerol, and free fatty acids remains unchanged in relation to the modulated severity of NASH despite their general elevation in high-fat fed foz/foz mice compared with wild-type counterparts (Van Rooyen *et al.,* 2011). Based on a large body of data above, hepatic cholesterol could be considered as a possible underlying lipotoxic molecule in the liver disease.

1.3. Mechanisms of cholesterol toxicity

Patients with metabolic disease or fatty liver express high level of TG, LDL-C, VLDL-C and low level of HDL-C. Thus, cholesterol toxicity has been primarily studied in pancreatic β-cell since obesity is an important risk factor for type 2 diabetes. Cholesterol treatment induced insulin resistance, mitochondrial dysfunction, oxidative stress, and apoptosis in MIN6 cells, βTC3, 832/13 INS-1 insulinoma cells and primary pancreatic cell (Carrasco-Pozo *et al.*, 2015; Hao *et al.*, 2007; Lee *et al.*, 2011; Simonen *et al.*, 2011; Zhao *et al.*, 2010). However, expression of glucose-regulated protein78 and CCAAT-enhancer-binding protein homologous protein was not altered after cholesterol treatment in MIN6 cells (Simonen *et al.*, 2011). Cholesterol toxicity was also investigated in depth in smooth muscle cells and macrophages, as they are the site of cardiovascular disease development. ER stress, destabilization of mitochondrial membrane permeability were commonly involved in toxic mechanism observed in smooth muscle cell (Kedi *et al.*, 2009; Rong *et al.*, 2003; Xu *et al.*, 2010). Interestingly, rapamycin treatment was reported to attenuate cholesterol-induced ER and mitochondrial stress (Xu *et al.*, 2010). In macrophage, cholesterol treatment caused both Fas ligand activation and mitochondrial apoptosis represented by activation of caspase-9 and translocation of cytochrome C and bcl-2-associated X protein (Yao and Tabas, 2001). On the contrary, although growing evidence indicates that free cholesterol accumulation is seen in experimental and human NASH, direct impact of cholesterol on liver cells has been barely studied in vitro. Based on previous studies, **Figure 1** depicts graphical abstract of possible toxic mechanisms induced by excess hepatic cholesterol. Activation of cholesterol de novo synthesis, increased cholesterol de-esterification, decreased cholesterol export and decreased bile acid synthesis are reported to contribute to

disruption of hepatic cholesterol homeostasis. Resulting accumulation of cholesterol is found to be in associated with the pathogenesis of NAFLD/NASH. FC accumulation activates intracellular signaling pathways in Kupffer cells and stellate cells, triggering inflammation and fibrogenesis. In hepatocytes, FC accumulation induces mitochondrial dysfunction, ER stress and ultimately apoptosis. Although ER stress and mitochondrial dysfunction are highlighted for their contribution in **Figure 1**, ER stress still remains controversial. An in vitro study using primary mouse hepatocyte incubated with LDL-C showed no alteration in CCAAT-enhancer-binding protein homologous protein and glucose-regulated protein78 protein level (Gan *et al.*, 2014). Also, multiple experimental models showed that FC accumulation in mitochondria sensitized hepatocytes to tumor necrosis factor α leading to mitochondrial GSH depletion whereas FC distribution in ER and plasma membrane did not cause ER stress or alter tumor necrosis factor signaling (Mari *et al.*, 2006).

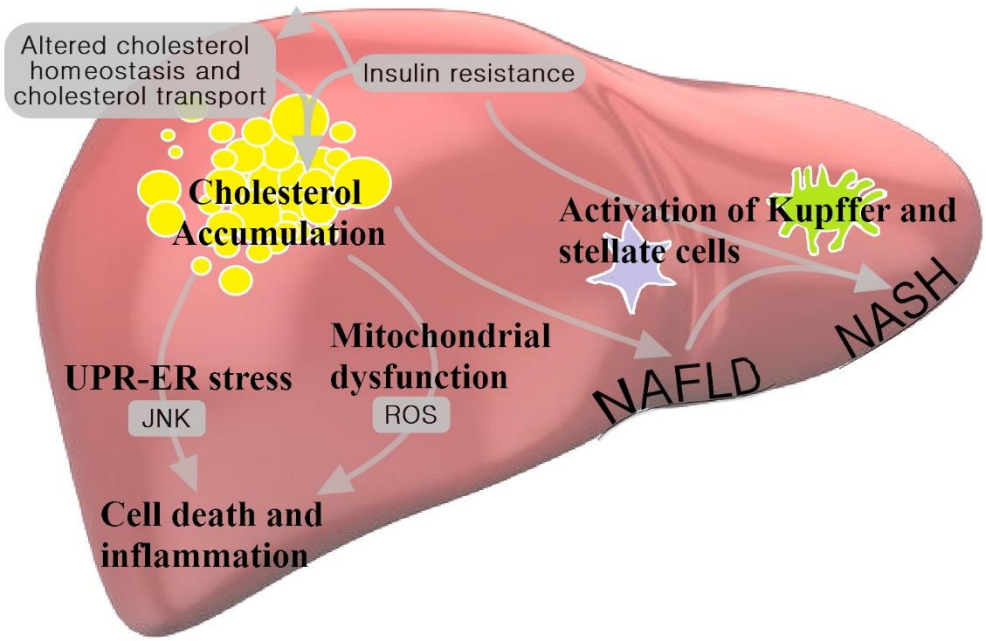

Figure 1. Liver injury triggered by cholesterol accumulation

(Arguello *et al.*, 2015) ER, Endoplasmic reticulum; JNK, c-Jun N-terminal kinase; NAFLD, non-alcoholic fatty liver disease; NASH, non-alcoholic steatohepatitis; ROS, reactive oxygen species; UPR, unfolded protein response

2. Autophagy as a house keeping system

2.1. The roles and the process of autophagy pathway

Autophagy (Greek for “self-eating) is a process by which cytoplasmic materials including proteins, lipids, and even organelles, reach lysosomes for degradation (Mizushima *et al.*, 2010). Three different types of autophagy are described: macroautophagy, chaperone-mediated autophagy and microautophagy. Of these classification, macroautophagy, herein simply referred to as autophagy, is the major form of autophagy and is conserved from yeast to mammals. This type of autophagy is mediated by a special vesicular organelle termed autophagosome. Chaperone-mediated autophagy requires chaperone proteins which facilitates direct translocation of cytosolic proteins across the lysosomal membrane. Microautophagy occurs through inward invagination of lysosomal membrane which enables delivery of a fraction of cytoplasm into the lysosomal lumen.

Autophagy, as a major degradation system, exerts distinct functions such as turnover of bulky cellular constituents, maintenance of intracellular homeostasis, antigen presentation, and cell death (Cecconi and Levine, 2008; Deretic *et al.*, 2013). Under basal conditions, cellular autophagic activity is usually kept at low, but can be sharply upregulated by numerous stimuli, such as starvation, hypoxia, energy depletion, ER stress, pharmacological agents, innate immune signals, and diseases such as bacterial, viral, and parasitic infections (Deretic *et al.*, 2013; Mizushima *et al.*, 2010). Conversely, autophagy suppression is often associated with certain disease, including cancers, neurodegenerative disorders, infectious diseases, and a decline in autophagy function is a hallmark of aging (Deretic *et al.*, 2013; Mizushima *et al.*, 2010). In an in vitro experiment using HeLa cells, when autophagy is pharmacologically inhibited by 3-

methyladenine, chloroquine, bafilomycin A1, or monensin, the activation of caspase-3 was observed, and nutrient depletion increased the level of the activation (Boya *et al.*, 2005).

Autophagy proceeds through several stages in which specific regulatory proteins and complexes are required (**Fig. 2**). In the initiation or nucleation stage, isolation membrane, also called phagophore or preautophagosomal structure, is formed from preexisting plasma or organelle membranes. This stage requires the activation of UNC51-like kinase (ULK) complex and the class III phosphatidylinositol 3-kinase (PI3K) complex. ULK complex consists of ULK1/2, autophagy-related gene protein (Atg) 13, FAK family kinase interacting protein of 200 kDa and Atg101 (Kaur and Debnath, 2015). Class III PI3K complex is composed of vacuolar protein sorting34, along with its regulatory subunits Atg14L, vacuolar protein sorting15 and beclin1 (Kaur and Debnath, 2015). In the elongation stage, the Atg12-Atg5-Atg16L complex facilitates the addition of phosphatidylethanolamine group to the microtubule-associated protein 1 light chain 3 (LC3). The LC3-II formed is then specifically associated with autophagosomes, and the phagosomal structure closes, enclosing a small portion of cytoplasm. Finally, the autophagosome fuses with lysosomes, leading to formation of the autolysosome. After fusion, delivered V+-ATPases and lysosomal hydrolases cause acidification and degradation of its contents.

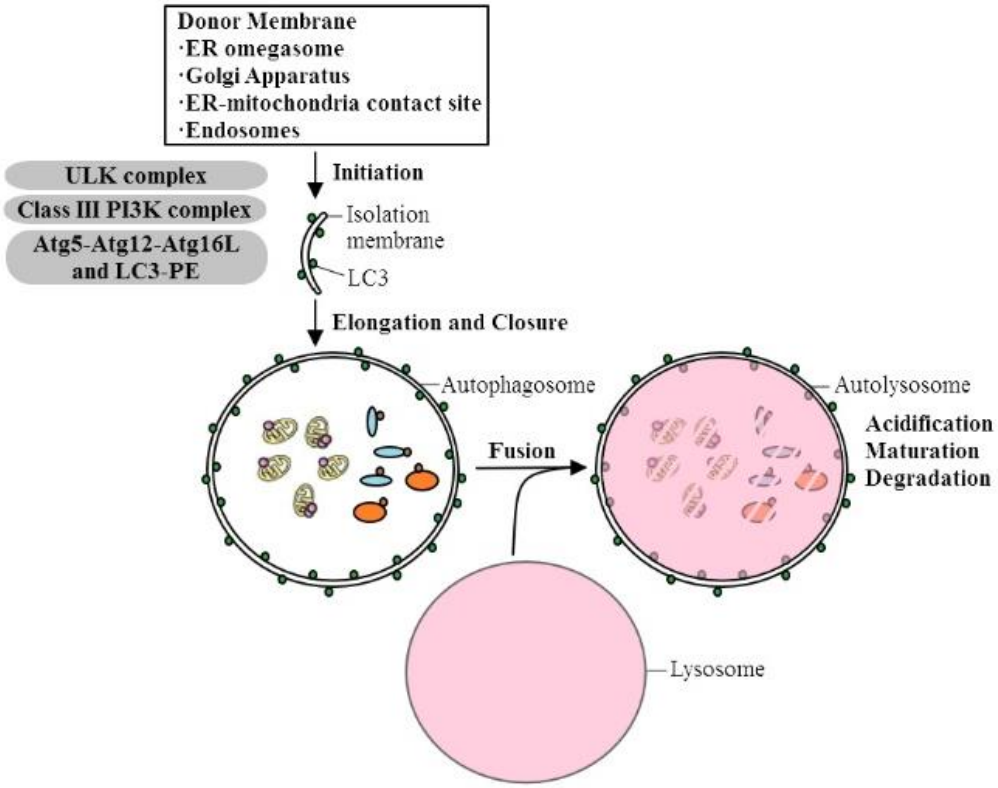

Figure 2. The process of macroautophagy

(Deretic *et al.*, 2013; Kaur and Debnath, 2015) Atg, autophagy related gene; LC3, microtubule-associated protein light chain 3; PE, phosphatidylethanolamine; PI3K, phosphatidylinositol 3-kinase

2.2. Markers for monitoring autophagy

In mammalian cells, most of the Atg proteins, for example, ULK1/2, Atg13, FIP200, Atg101, Beclin 1, Atg14, LC3, Atg12, Atg16L, are observed on isolation membranes but not on complete autophagosomes (Longatti and Tooze, 2009). Only LC3, a mammalian homolog of yeast Atg8, is known to exist on autophaogomes, which makes this protein serve as a widely used marker for autophagosomes. However, the level of LC3 protein should be interpreted with caution because autophagosome accumulation may represent either autophagy induction or, oppositely, suppression of later steps in the autophagy pathway after autophagosome formation, given that the autophagosome is a mere intermediate structure in a dynamic pathway. Under normal conditions, basal autophagy occurs and when autophagy is induced, all types of autophagic structures, such as isolation membrane, autophagosome, and autolysosome, increase. When autophagy is suppressed at any step upstream, none of the autophagic structures are generated. When autophagy is suppressed at any step after complete closure of the autophagosome, only autophagosomes accumulate. Thus, the simple determination of numbers of autophagosomes is not sufficient to estimate autophagic activity. Rather, measuring autophagic flux is a more reliable indicator of autophagic activity. Autophagic flux encompasses the comprehensive process of autophagy from autophagosome synthesis to degradation of autophagic substrates inside the lysosome. One of the principal methods to measure autophagic flux is monitoring of LC3 turnover, which is based on the fact that LC3-II is degraded in autolysosomes. Treating cells with lysosomal inhibitors such as ammonium chloride, chloroquine, or bafilomycin A1, which inhibit acidification inside the lysosome or autophagosome-lysosome fusion or with inhibitors of lysosomal proteases such as E64d and pepstatin A results in LC3-II accumulation (**Fig.**

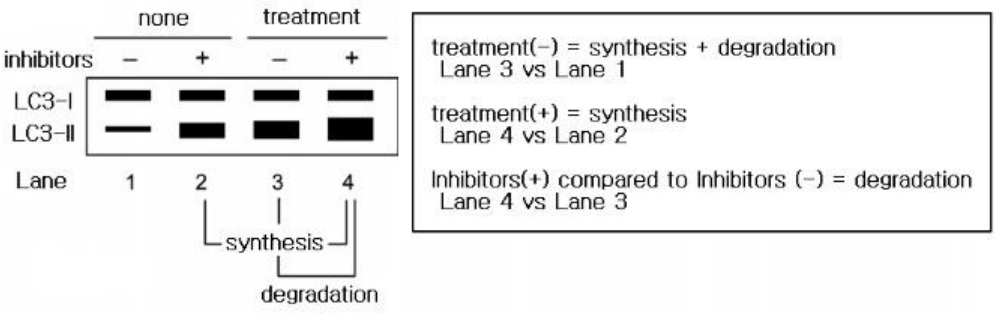

Figure 3. Interpretation of LC3 immunoblotting.

(Rubinsztein *et al.*, 2009)

3). Therefore, net amount of degradation, or autophagic flux can be estimated by measuring the differences in the amount of LC3-II between samples in the presence and absence of lysosomal inhibitors. The difference in the levels of LC3-II in the presence or absence of lysosomal inhibitor reflects the net amount of this protein delivered to the lysosomes. If a compound raises LC3-II levels in the absence of inhibitor, but there is no further rise in its presence, then it can be inferred that there is a blockage in LC3-II degradation (Rios-Marco *et al.,* 2015; Rubinsztein *et al.,* 2009). The p62 protein, also known as sequestome1, can also be used to monitor autophagic flux. The p62 protein serves as a link between LC3 and ubiquitinated substrates and is efficiently degraded by autophagy. Thus, decreased autophagic flux correlates with an increased p62 level, and vice versa, increased autophagic flux correlates with a decreased p62 level (Zhang *et al.*, 2013). However, unlike LC3, p62 has some potential experimental pitfalls by nature. P62 can be also degraded by ubiquitin-proteasome system and can interact with several other signaling molecules other than LC3 (Moscat and Diaz-Meco, 2009). Also, it can be transcriptionally upregulated under certain conditions (Nakaso *et al.*, 2004). Thus, measurement of the p62 level is recommended to be performed along with other methods such as LC3-II turnover assay (Zhang *et al.*, 2013).

Currently, it is not clear whether autophagic activity per se can be transcriptionally regulated or not. Thus, mRNA levels of LC3 and other autophagy genes are not recommended to measure autophagic activity, although they may be transcriptionally upregulated in response to stress conditions that induce autophagy. In fact, Atg proteins are constitutively expressed in sufficient amounts, so their posttranslational modifications and/or associations with other members of the autophagic machinery are considered more important indicators of autophagic activity (Mizushima *et al.*, 2010).

Lastly, although the number and activity of lysosomes are commonly used as markers for autophagic activity, they are not a reliable general indicator of autophagy in mammalian cells. They may work well in *Drosphila*, but for mammalian cells, the use of LysoTracker, acridine orange or monodansylcadaverine is not recommended (Mizushima *et al.*, 2010).

3. Aims of the study

Given the strong association between NAFLD progression and hepatic cholesterol accumulation, cholesterol may be a possible lipotoxic molecule leading to NAFLD. Thus, this study was conducted to determine cholesterol lipotoxicity in hepatocytes using cholesterol overloaded HepG2 cells. Precisely, whether dysregulated cholesterol homeostasis alters autophagic activity and contributes to apoptosis was investigated.

Ⅱ. Materials and Methods

1. Cell culture

A human, well differentiated hepatoblastoma cell line, HepG2 cells chosen in this study have been shown to retain a wide variety of liver-specific metabolic functions including cholesterol and triglyceride metabolism (Javitt, 1990; Molowa and Cimis, 1989). HepG2 cells were obtained from American Type Culture Collection (ATCC, USA) and were cultured in Dulbecco's modified Eagle's medium (DMEM; Welgene Biotech, South Korea) supplemented with 10% heat inactivated fetal bovine serum (Welgene Biotech, South Korea), 1% penicillin-streptomycin (Welgene Biotech, South Korea). Cell cultures were maintained in a humidified incubator in 5% CO2 atmosphere at 37 °C.

2. Cholesterol overloading

Cholesterol was delivered to HepG2 cells by cholesterol:methyl-β-cyclodextrin complex which contains approximately 45 mg of cholesterol/g (Sigma, USA). Cyclodextrins are water soluble cyclic oligosaccharides consisting of α-(1-4)-linked D-glycopyranose units, which contain a hydrophobic cavity capable of encapsulating hydrophobic molecules, in this case, cholesterol (Zidovetzki and Levitan, 2007). Cholesterol:methyl-β-cyclodextrin has been frequently chosen to manipulate the cholesterol contents within cells (Christian *et al.*, 1997; Garbarino *et al.*, 2012; Rong *et al.*, 2003; Vengrenyuk *et al.*, 2015; Wang *et al.*, 2015; Xu *et al.*, 2010). Cholesterol:methyl-β-cyclodextrin stock was prepared by dissolving the powder in water. HepG2 cells were plated on the culture dish until the cells reached 70-80% confluence and the serum in media was deprived for 12 h. To load excess cholesterol, the monolayer

was incubated with 25 or 50 µg/mL cholesterol in the culture media for 24 h. All treatment concentrations indicated were calculated based on cholesterol weight. Same volume of water loaded cells as cholesterol treated cells were used as vehicle control.

3. Light microscopy

HepG2 cells were equally seeded in 96-well plate (Corning Inc., USA) and then treated with cholesterol for 12 h. The cells were washed gently three times with phosphate buffered saline (PBS). The morphology of HepG2 cells was observed under light microscope (Olympus CKX41, Japan).

4. Total cholesterol mass quantification

Cellular total cholesterol (TC) was quantitated by a modification of previously described methods. Briefly, cells were harvest in PBS and sonicated. The protein content of the homogenate was measured using a protein assay kit (Bio-Rad, USA). 300 µL homogenate containing 1 mg/mL protein was prepared, mixed with 1.2 mL of chloroform/methanol (2:1, v:v), and incubated overnight at 4°C. Thereafter, 240 µL of 0.88% KCl was added for aggregation of non-lipid contents and centrifuged at 1000×g for 15 min at 4°C. The bottom layer was obtained, aliquoted. The solvent was then evaporated from aliquots, and the lipid residue was solubilized in the assay buffer in the same volume evaporated. The amount of TC was determined by enzymatic colorimetric methods using the commercial kits according to the manufacturer's instructions (Asan Pharmaceutical Co, South Korea). Cellular cholesterol results are reported as µg of TC per mg cell protein.

5. Lipid peroxidation measurement

Lipid peroxidation was determined by measuring thiobarbituric acid reactive substances (TBARS) in HepG2 cells as described by Ohkawa *et al* (Ohkawa *et al.*, 1979). Briefly, cells were collected in homogenizing buffer [Homogenizing buffer; 154 mM KCl, 50 mM Tris-HCl, 1mM EDTA (pH7.4)] and lysed by sonication. Resultant whole cell lysates were mixed with 8.1% SDS, 10% acetic acid, 0.8% thiobarbituric acid (TBA) followed by 1 h incubation in a 95℃ water bath. After development of the color, tubes were immediately cooled on ice for termination of the reaction. 1-butanol:pyridine mixture (15:1, v/v) was then added, vortexed vigorously and centrifuged at 4000 rpm for 20 mins to obtain supernatant. The absorbance of the supernatant was measured at 532 nm using UV-visible Spectrophotometer (Molecular Device, USA). Absorbance readings at 532nm were converted to TBARS values (nmol/mg protein), using 1,1,3,3-tetraethoxypropane as a reference standard.

6. Detection of Reactive Oxygen Species Generation

Oxidation of 2′,7′-dichlorodihydrofluorescein diacetate (H_2DCFDA; Sigma, USA) occurs almost exclusively in the cytosol, and generates a fluorescence that is proportional to reactive oxygen species (ROS) generation. Thus, the presence of ROS was measured using the probe. Briefly, HepG2 cells were cultured in phenol red free DMEM with 10% FBS in Lab-TEK TekII chamber slides (Fisher Scientific, USA) and after reaching 60-70% confluency, cells were treated with either 50 μM H_2O_2 or 50 μg/mL cholesterol in phenol red free, serum free DMEM for 24 h. After treatments, cells were washed twice with PBS and incubated with 25 μM of H_2DCFDA dye for 30 min at 37°C in dark. Following incubations, cells were washed once with PBS and immediately examined

under Axio Observer Z.1 inverted light microscope (Carl Zeiss, Germany) equipped with fluorescein isothiocyanate filter. Fluorescent photos were taken once per well due to the photosensitivity of the H_2DCFDA reagent observed under fluorescent wavelengths.

7. Cell viability determination

Cell viability was quantified using a 3-(4,5-dimethylthiazol-2-yl)-2,5-diphenyltetrazolium (MTT) assay by measuring mitochondrial dehydrogenase activity. The assay is based on the ability of living cells to convert water-soluble MTT into insoluble purple formazan that is proportional to the number of respiring cells. HepG2 cells were seeded at the density of 5×10^5 cells/well in a 96-well plate and allowed to attach for 24 h. After treatments, cells were incubated with final concentration of 0.5 mg/mL of MTT in DMEM for 1 h at 37°C. The media was then aspirated with little disturbance of the formazan crystals, which were later solubilized in DMSO for a further 1h before measuring the optical density. The absorbance was read at 540 and 690 nm in a microplate reader (Bio-Rad, USA). The corrected absorbance was obtained by subtracting the 690 nm value from the 540 nm value for background correction, eliminating unspecific signal. Relative cell viability was calculated as percentage of control.

8. Total protein extraction

Unless otherwise noted, after treatment, cells were rinsed with ice cold PBS and lysed in the ice-cold lysis buffer containing 50 mM Hepes-KOH (pH 7.5), 150 mM NaCl, 1 mM EDTA (pH 8.0), 2.5 mM EGTA (pH 8.0), 1mM NaF, 10mM β-glycerophosphate, 0.1 mM Na_3VO_4, 1 mM DTT, 0.1% Tween-20, 10% glycerol, protease inhibitor cocktail

(Sigma, USA). Lysates were centrifuged at 10000×g for 30 min at 4°C. Supernatant containing protein content was collected and measured using protein assay kit (Bio-Rad, USA).

9. Protein solubility fractionation

Detergent insoluble fraction was collected as previously described (Park *et al.*, 2014) with little variation. Briefly, cells were lysed in a lysis buffer containing 0.1% Triton X-100 instead of 0.1% Tween-20. Cell lysates were centrifuged at 15,000 r.p.m for 15 min at 4°C to obtain supernatants. Pellets were resuspended in a lysis buffer containing 1% Triton X-100, the procedure being repeated. Lastly, detergent insoluble pellets were solubilized in a lysis buffer containing 2% SDS.

10. Western blotting

For immunoblotting, equal amounts of protein were boiled in SDS sample buffer for 5 min, loaded into the lanes of SDS-PAGE gel, separated and then transferred to polyvinylidene fluoride membrane. After blocking, with either 5% non-fat milk or 5% BSA, membranes were probed with specific primary antibodies and subsequently incubated with HRP-linked secondary antibodies. The immunoreactive protein bands were visualized by chemiluminescent using HRP substrate (Millipore, USA) with exposure to X-ray film (Fuji, Japan). The bands intensities were quantified with the Quantity one software (Bio-Rad, USA). Primary antibodies were obtained as followings; (nonerythroid) α-spectrin (Chemicon, USA), Ub (Santa Cruz Biotechnology, USA), Beclin-1 (Santa Cruz Biotechnology, USA), Caspase-3 (Cell Signaling, USA), KDEL (Enzo Life Sciences, USA), LC3 (Novus Biology, USA), p-JNK (Cell Signaling, USA),

JNK (Cell Signaling, USA), p62 (Santa Cruz Biotechnology, USA), Caspase-9 (Cell Signaling, USA), p-AMPK (Cell Signaling, USA), AMPK (Cell Signaling, USA).

11. Statistical analysis

All data were analyzed using SPSS software (ver. 22.0, SPSS Inc., USA). The data were analyzed by one-way analysis of variance (ANOVA). Where appropriate, post hoc comparisons were made by Duncan's multiple range test. Student's t-test was used for two-group comparison. The data were reported as means ± SEM, and differences were considered significant at $P < 0.05$.

Ⅲ. Results

1. Incubation with cholesterol increases cellular cholesterol content in HepG2 cells

Cells were exposed to the indicated concentrations of cholesterol for 24h and the cellular lipid content was measured (**Fig. 4**). As a result, incubation with 50 μg/mL cholesterol raised intracellular cholesterol level compared with control cells.

In a human study (Puri *et al.*, 2007), hepatic FC level of control group was reported to be approximately 20 μg/mg protein, and this value increased by 1.7-fold in the NASH group. Another previous study (Wouters *et al.*, 2008) using LDLR−/− male mice, which bear many characteristics of human NAFLD/NASH, showed that liver TC levels reached approximately 80 μg/mg protein with signs of hepatic inflammation after 7 days of a high-fat, high-cholesterol diets. Hepatic TC levels of chow diet group in this study was approximately 30 μg/mg protein and no increase in liver TG levels was shown. Thus, measured quantity of accumulated cholesterol seems to be physiologically relevant to hepatic cholesterol level observed in human and experimental liver disease model.

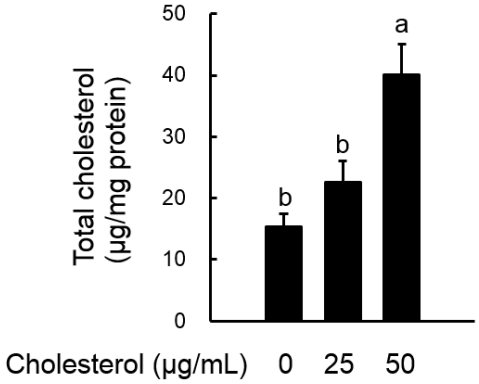

Figure 4. Intracellular lipid contents after cholesterol treatment in HepG2 cells

Cells were incubated with the indicated concentration of cholesterol in media without serum for 24 h and intracellular total cholesterol. Bars represent the means ± SEM (n = 4) and bars with different superscripts are significantly different at $P < 0.05$.

2. Cholesterol overloading suppresses cell viability and induces apoptosis in HepG2 cells

Previous studies reported cholesterol induced cytotoxity in several cell types. Thus, to determine whether cholesterol reduces cell viability in hepatocytes, HepG2 cells were exposed to the indicated concentrations of cholesterol and the cell viability was measured by MTT assays. As a result, dose-dependent reduction of cell viability was observed after 24 h. Cell population decreased following the incubation in cholesterol (**Fig.5, Fig.6**). Non-erythroid spectrin (also called fodrin) is a major component of cortical cytoskeleton that has binding sites for several proteins, and it consists of α and β subunits (Cryns *et al.*, 1996). Proteolysis of fodrin has been detected during apoptosis of various cell lines and inhibited under conditions where apoptosis was prevented. Previous study (Martin *et al.*, 1995) suggested that given its role as a major component of the plasma membrane-associated cytoskeleton, membrane blebbing in apoptosis may be at least partly due to disruption of the fodrin network. Thus, to confirm occurrence of apoptosis, HepG2 cells were exposed to the cholesterol for 24h and the cleavage of α-fodrin was determined by Western blotting. Decreases in the intact form (280kDa) of non-erythroid spectrin by cholesterol was observed (**Fig.7A**). Cleaved caspase-3, an effector molecule commonly involved in apoptosis, was also increased as dose of cholesterol increased (**Fig.7B**).

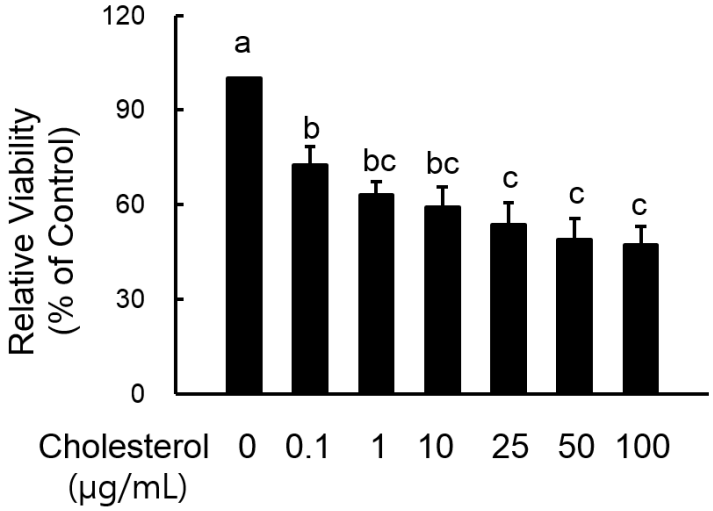

Figure 5. Effects of cholesterol on cell viability in HepG2 cells

Cells were incubated with the indicated concentration of cholesterol in media without serum and the cell viability was measured by MTT assay. Bars represent the means ± SEM (n = 3) and bars with different superscripts are significantly different at $P<0.05$.

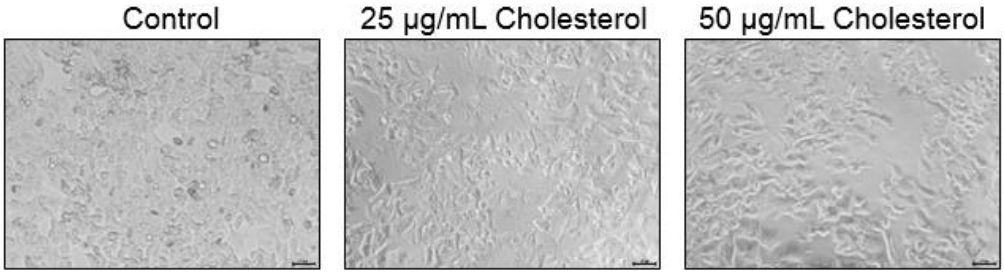

Figure 6. Effects of cholesterol on cell populations in HepG2 cells

The microscopic images of HepG2 cells after treatment of cholesterol for 24 h were photographed. The cellular population was observed using inverted light microscopy. Scale bars = 50 µm. Images are representative of three independent experiments.

(A)

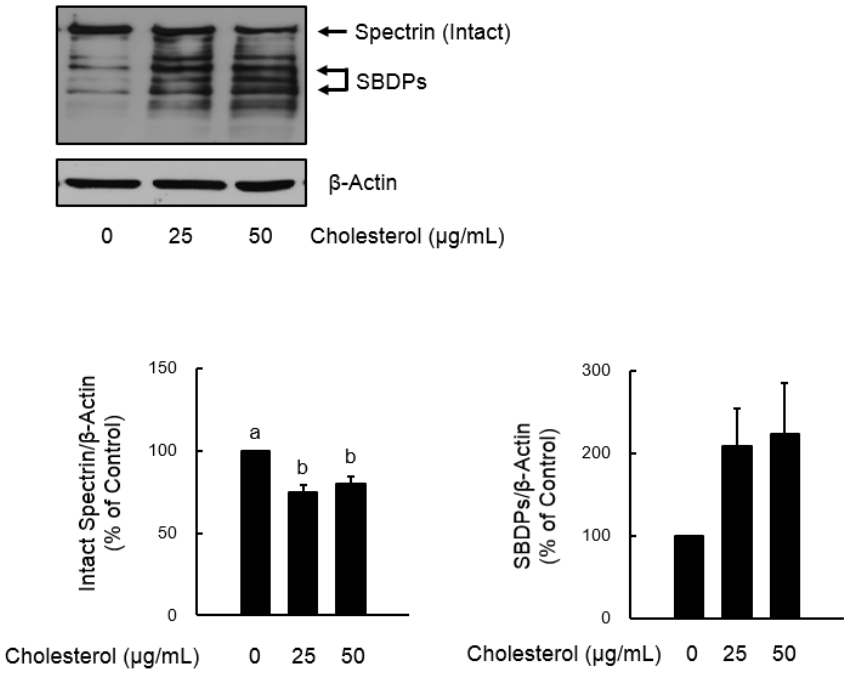
Spectrin (Intact)
SBDPs
β-Actin
0 25 50 Cholesterol (μg/mL)
Intact Spectrin/β-Actin (% of Control)
150
100
50
0
a
b
b
Cholesterol (μg/mL) 0 25 50
SBDPs/β-Actin (% of Control)
300
200
100
0
Cholesterol (μg/mL) 0 25 50

(B)

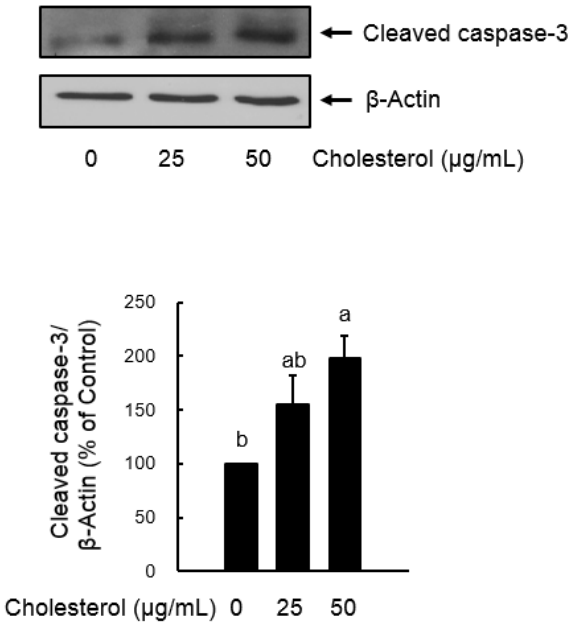
Cleaved caspase-3
β-Actin
0 25 50 Cholesterol (μg/mL)
Cleaved caspase-3/ β-Actin (% of Control)
250
200
150
100
50
0
b
ab
a
Cholesterol (μg/mL) 0 25 50

Figure 7. Effects of cholesterol on apoptosis in HepG2 cells

α-Spectrin and cleaved caspase-3 were detected by immunoblotting and quantitated. Cells were treated with 25 μg/mL or 50 μg/mL cholesterol in media without serum for 24 h after serum deprived overnight. The total protein lysates were subjected to SDS-PAGE and transferred to PVDF membrane. (A) Representative α-spectrin and β-actin immunoblots are shown. The ratio of intact spectrin and SBDPs are expressed as percentage of the control value. Each bar represents means ± SEM (n = 6). (A) Representative cleaved caspase-3 and β-actin immunoblots are shown. The ratio of cleaved caspase-3 is expressed as percentage of the control value. Each bar represents means ± SEM (n = 3). Bars with different superscripts are significantly different at $P < 0.05$.

3. Cholesterol overloading results in increases of autophagic markers in HepG2 cells

Autophagy is regulated by autophagy specific genes (Atg) including *Beclin1*, the mammalian orthologue of Atg*6* in yeast. Beclin 1 localizes to the trans-Golgi network, belongs to the class III PI3K complex and participates in autophagosome formation. LC3, mammalian homolog of yeast Atg8, exists in two forms: cytosolic-associated LC3-I and membrane-bound LC3-II which is a proteolytic derivative of the former (16 and 14 kDa, respectively). LC3-II can be used to estimate the abundance of autophagosomes before they are destroyed through fusion with lysosomes (Boya *et al.*, 2005). Adaptor protein p62 binds to LC3 and facilitates the autophagic degradation of ubiquitinated protein aggregates in lysosomes. Both p62 and LC3 are routinely used as biomarkers to monitor the level of autophagy.

Previous study reported that autophagy showed a protective effect against FC overload-induced death in smooth muscle cell (Xu *et al.*, 2010). To determine whether autophagy is activated by cholesterol treatment in HepG2, autophagy markers aforementioned were detected (**Fig.8**). Treatment of cholesterol strongly induced the increase of LC3-II and p62 protein levels. Beclin-1 remained unchanged.

(A)

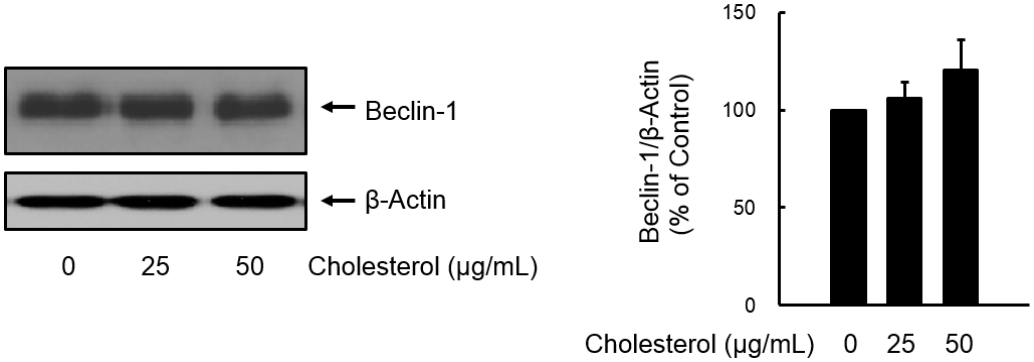
Beclin-1
β-Actin
0
25
50
Cholesterol (μg/mL)
Beclin-1/β-Actin
(% of Control)
150
100
50
0
Cholesterol (μg/mL) 0 25 50

(B)

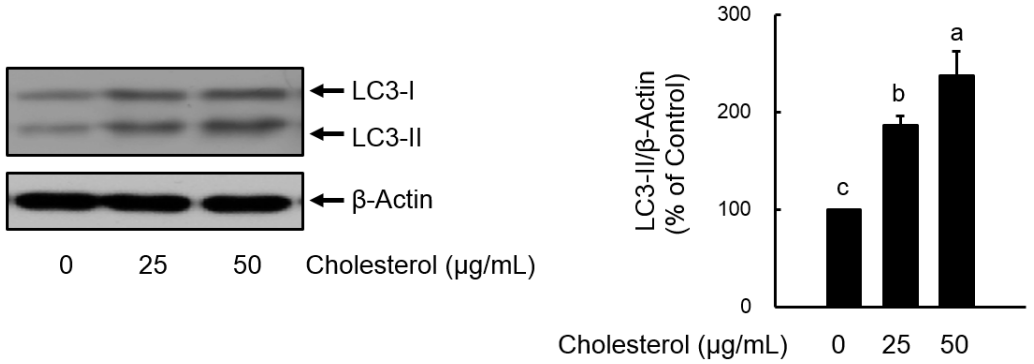
LC3-I
LC3-II
β-Actin
0
25
50
Cholesterol (μg/mL)
LC3-II/β-Actin
(% of Control)
300
200
100
0
a
b
c
Cholesterol (μg/mL) 0 25 50

(C)

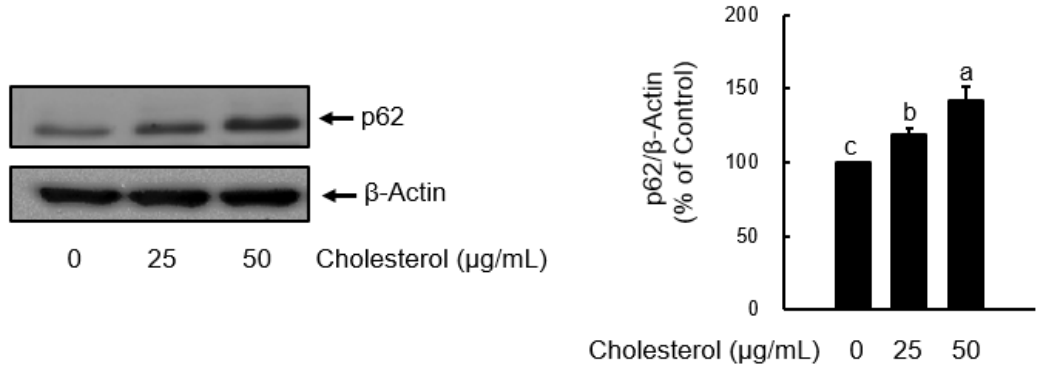
p62
β-Actin
0
25
50
Cholesterol (μg/mL)
p62/β-Actin
(% of Control)
200
150
100
50
0
a
b
c
Cholesterol (μg/mL) 0 25 50

Figure 8. Effects of cholesterol on autophagic in HepG2 cells.

Relative expression of autophagic markers were detected by immunoblotting and quantitated. Cells were treated with 25 μg/mL or 50 μg/mL cholesterol in media without serum for 24 h after serum deprived overnight. (A) Representative LC3 immunoblots are shown. Relative expression of LC3-Ⅱ was quantified and expressed as percentage over the control value. Each bar represents means ± SEM (n = 6). (B) Representative Beclin-1 immunoblots are shown. Relative expression of Beclin-1 was quantified and expressed as percentage over the control value. Each bar represents means ± SEM (n = 5). (C) Representative p62 immunoblots are shown. Relative expression of p62 was quantified and expressed as percentage over the control value. Each bar represents means ± SEM (n = 4). Bars with different superscripts are significantly different at $P < 0.05$.

4. Autophagic flux is reduced in cholesterol overloaded HepG2 cells.

Cholesterol overloading increased LC3-II and p62 protein levels as shown in **Fig.8**. Since increased p62 protein level correlates decreased autophagic flux (Zhang *et al.*, 2013), LC3-II level was measured in the presence/absence of lysosomal inhibitor chloroquine (**Fig. 9A)**. Lysosomal lumen alkalizer chloroquine is frequently employed to investigate autophagic flux by block autophagic progress by impairing lysosomes. **Figure 9B** illustrates that cholesterol treatment for 24 h indeed lowered the net amount of LC3-Ⅱ delivered to the lysosomes.

To determine the functional importance of autophagy inhibition and lysosomal impairment in HepG2 cells, ubiquitinated proteins and p62 proteins were measured. The two main intracellular protein degrading systems, ubiquitin-proteasome and autophagy-lysosome pathways, are closely engaged. It is well known that ubiquitinated proteins target p62 for autophagic degradation, and disruption of the autophagy-lysosome pathway results in ubiquitinated aggregates (Korolchuk *et al.*, 2009; Yu *et al.*, 2013). Compared to control group, levels of p62 and ubiquitinated proteins increased after exposure to cholesterol for 24 h. Moreover, further autophagy inhibition increased levels of proteasome substrates (**Fig. 9C**).

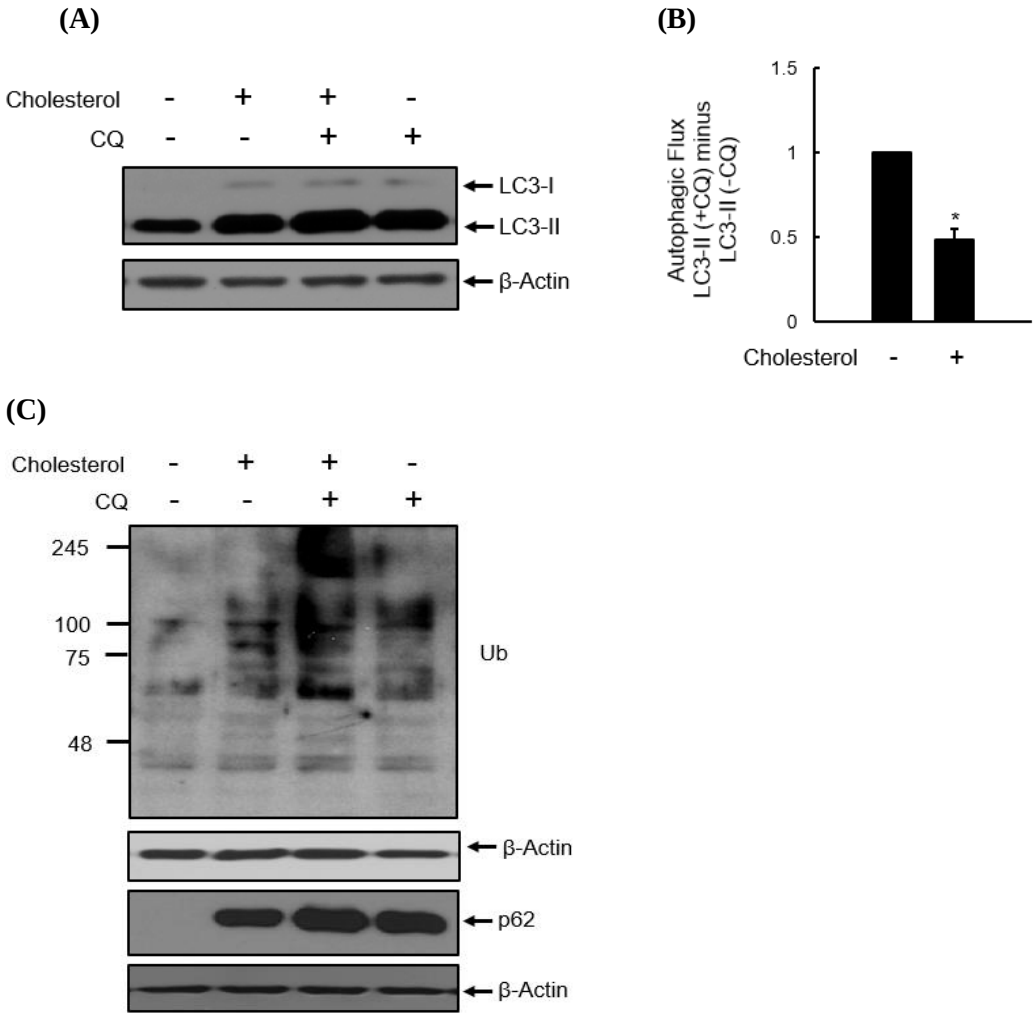

Figure 9. Cholesterol-induced reduction in autophagic flux in HepG2 cells

Cells were treated with 50 µg/mL cholesterol in the presence or the absence of 10 µM chloroquine in media without serum for 24 h after serum deprived overnight. PBS treatment was used as the vehicle control. (A) Representative LC3 immunoblots of four independent experiments are shown. (B) Effect of cholesterol on the autophagic flux in HepG2 is displayed as a diagram. Autophagic flux was determined by the strength of LC3-II accumulation in a 24 h treatment period with chloroquine. Therefore, normalized LC3-II levels in the absence of chloroquine were subtracted from the corresponding levels obtained in the presence of chloroquine. Values are expressed as means ± SEM (n = 4) and asterisk indicates statistical significance. (C) Representative ubiquitinated proteins and p62 immunoblots of four independent experiments are shown.

5. Attenuation of autophagic flux by cholesterol is insufficient to trigger systemic cell death in HepG2 cells.

Autophagy inhibition is known to induce caspase-3 activation and ultimately apoptosis (Boya *et al.*, 2005). As observed in **Figure 9**, 10 µM chloroquine treatment resulted in similar quantity of LC3-II, p62 and ubiquitinated protein accumulation as 50 µg/mL cholesterol treatment. Thus, cell viability level was compared between the two treatments to measure to what extent blockage of autophagic flux contributes to cholesterol induced caspase-3 activation (**Fig. 10**). As a result, 10 µM chloroquine treatment had little impact on cell viability level, from which can be inferred that blockage of autophagic flux is not enough to cause systemic cell death, unless other toxic mechanisms are involved.

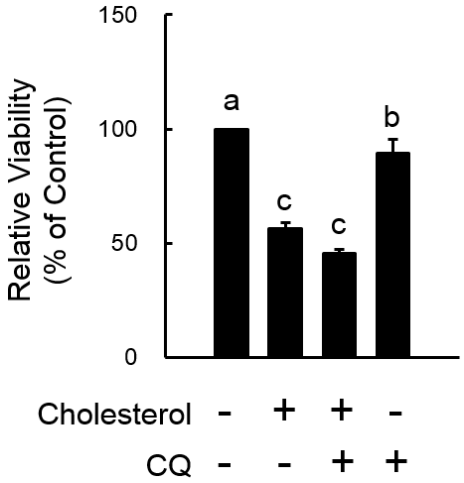

Figure 10. Effects of autophagy inhibition on cell viability in HepG2 cells.

Cells were incubated with 50 μg/mL cholesterol in the presence or the absence of 10 μM chloroquine in media without serum for 24 h after serum deprived overnight. PBS treatment was used as the vehicle control. The cell viability was measured by MTT assay. Bars represent the means ± SEM (n = 3) and bars with different superscripts are significantly different at $P < 0.05$.

6. Cholesterol overloading produces intracellular ROS and induces lipid peroxidation in HepG2 cells

ROS plays a key role in cell apoptosis. Therefore, generation of intracellular ROS by DCF, which is a probe oxidized by ROS to produce green fluorescence. **Figure 11A** shows that a significant increase in the ROS level (green fluorescence) appeared in cells treated with 50 µg/mL cholesterol for 24 h when compared with the control cells and even with positive control cells treated with 50 µM H_2O_2. In addition, as seen in the **Figure 11B**, cholesterol promoted production of lipid peroxidation. Previous studies have identified c-Jun N-terminal kinase (JNK) overactivation as an underlying mechanism of hepatocyte death from oxidant stress (Wang *et al.*, 2004; Wang *et al.*, 2010). Therefore, we determined the activation of JNK and observed an increase in phosphorylated form of JNK by cholesterol (**Fig.11C**).

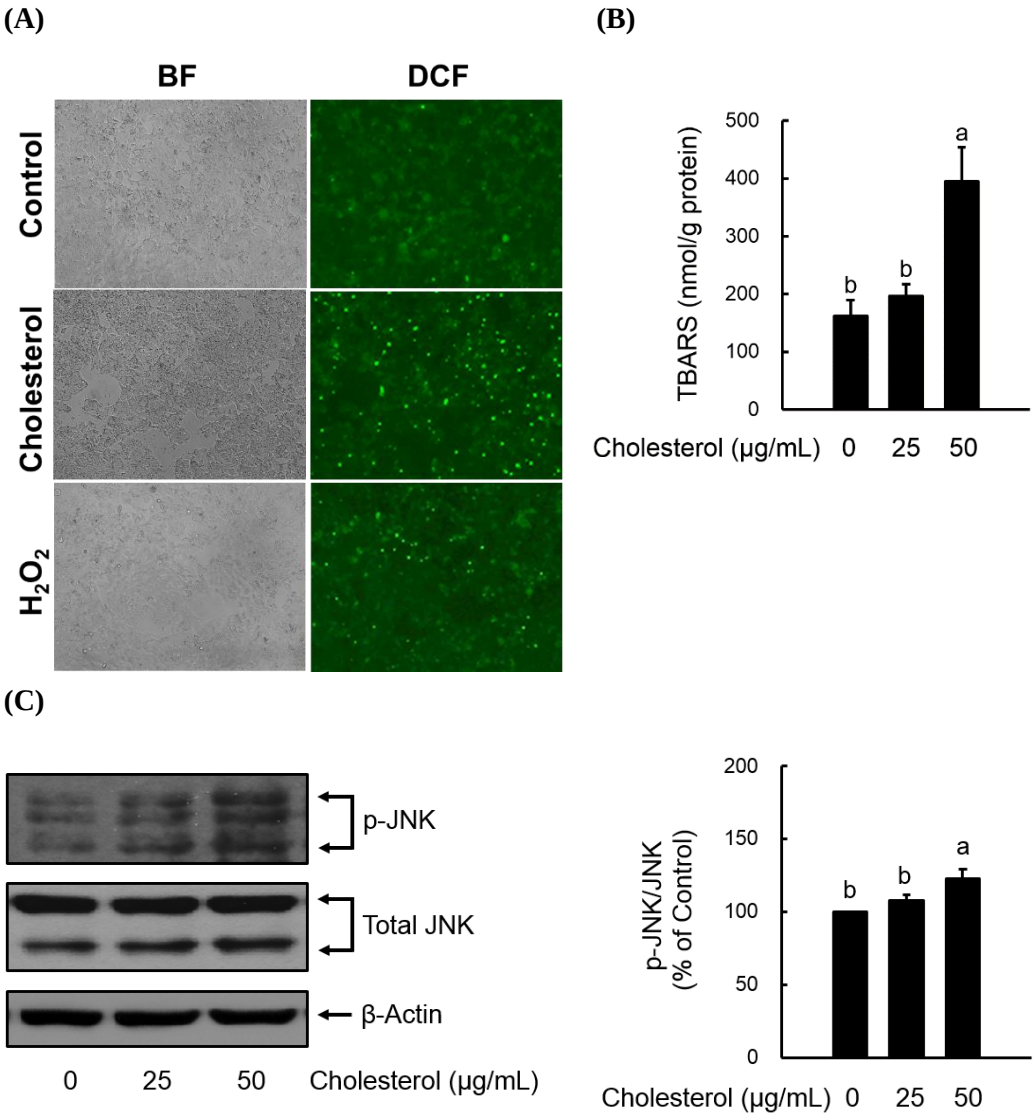
(A)
BF
DCF
Control
Cholesterol
H2O2
(B)
TBARS (nmol/g protein)
500
400
300
200
100
0
a
b
b
Cholesterol (μg/mL) 0 25 50
(C)
p-JNK
Total JNK
β-Actin
0 25 50 Cholesterol (μg/mL)
p-JNK/JNK (% of Control)
200
150
100
50
0
a
b
b
Cholesterol (μg/mL) 0 25 50

Figure 11. Effects of cholesterol on oxidative stress of HepG2 cells

(A) Either 50 μg/mL cholesterol or 50 μM H_2O_2 was treated for 24 h and intracellular ROS level was detected by observing Oxidation of H_2DCFDA. Representative of three brightfield (BF), H_2DCFDA (DCF) images from exact same time point are shown. (B) Cells were treated with 25 μg/mL or 50 μg/mL cholesterol in media without serum for 24 h after serum deprived overnight and lipid peroxidation was determined by measuring TBARS. Each bar represents the means ± SEM (n = 3). (C) Representative p-JNK immunoblots are shown. Relative expression of p-JNK was quantified and expressed as percentage over the control value. Each bar represents means ± SEM (n = 8). Bars with different superscripts are significantly different at $P < 0.05$.

7. Defective mitochondria is involved in cholesterol-induced cell death in HepG2 cells

Because hepatocyte free cholesterol lipotoxicity caused by JNK1-mediated mitochondrial injury (Gan *et al.*, 2014), we determined parameters of mitochondria toxicity. Following mitochondrial outer membrane permeabilization, various proteins are released from the mitochondrial intermembrane space and promote caspase activation and apoptosis. Cytochrome c binds apoptotic protease-activation factor 1, inducing its oligomerization and thereby forming apoptosome that recruits and activates an initiator caspase 9. Caspase 9 cleaves and activates executioner caspase 3 and caspase 7, leading to apoptosis (Tait and Green, 2010). Thus, cleavage of caspase 9 was detected to confirm mitochondrial damage. Mitochondrial damage results in insufficient production of ATP, leading to the activation of adenosine monophosphate-activated kinase (AMPK). Reduction of the ATP levels have severe consequences to the cell's function and health, since ATP mediates signal transduction, metabolism, active transport, DNA and RNA synthesis, and other critical pathways. Thus, phosphorylation status of Thr172 of AMPK was analyzed to indirectly investigate cellular ATP level. The result indicates that AMPK was significantly activated by cholesterol loading.

(A)

(B)

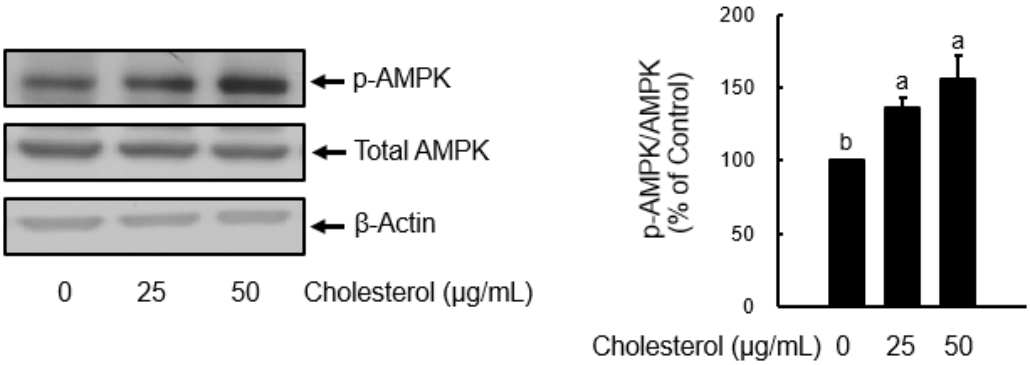

Figure 12. Effects of cholesterol on mitochondria in HepG2 cells

Cells were treated with 25 μg/mL or 50 μg/mL cholesterol in media without serum for 24 h after serum deprived overnight. (A) Representative cleaved caspase-9 immunoblots are shown. Relative expression of cleaved caspase-9 was quantified and expressed as percentage over the control value. Each bar represents means ± SEM (n = 4). (B) Representative p-AMPK immunoblots are shown. Relative expression of p-AMPK was quantified and expressed as percentage over the control value. Each bar represents means ± SEM (n = 4). Bars with different superscripts are significantly different at $P < 0.05$.

Ⅳ. Discussion

Lipotoxicity links ectopic lipid accumulation and cell death, and has been thought to be the main contributor to the progression of various diseases, such as obesity, diabetes, and NAFLD (Brookheart *et al.*, 2009). On the other hand, autophagy is essential for maintaining cellular homeostasis by preventing accumulation of damaged proteins and organelles. In this study, we examined whether cholesterol plays a role in hepatocyte lipotoxicity in relation to NAFLD pathology. For the first time, effects of hepatic cholesterol accumulation on the autophagic process were examined. Previously, there have been reports which investigated the toxic effects of cholesterol and its leading role on NAFLD development in vivo. However, tools to measure autophagic flux in vivo have been limited. Thus, no data is available despite compelling associations between cholesterol and pathological phenotype of NAFLD in terms of autophagy.

Herein, cholesterol treatment resulted in increases in LC3-II and p62 protein levels and concomitant increases in ubiquitinated proteins in HepG2 cells. Given that decreased autophagic flux correlates with an increased p62 level and vice versa (Zhang *et al.*, 2013), accumulation of LC3-II protein was suspected to be the results of decreased autophagosome clearance. This was confirmed by further investigations of autophagy pathway under cholesterol accumulation using a lysosomotropic agent chloroquine. LC3-II turnover assay using chloroquine revealed that autophagic flux was indeed reduced after cholesterol overloading. Consistently, associations between steatotic liver and defective autophagy have been reported in several studies. Accumulation of p62 proteins in cholesterol loaded HepG2 cells matches with the previous reports. For

instances, p62 protein was accumulated in the liver of Ob/Ob mice, implying deficiency in autophagic degradation in steatotic livers (Inami *et al.*, 2011). In NAFLD patients, p62 aggregation was correlated with serum alanine aminotransferase value and inflammatory activity by NAFLD score (Fukuo *et al.*, 2014). Therefore, in align with these previous reports, the present study suggests that cholesterol may be one of the causes of perturbation of autophagy in fatty liver. Accumulation of ubiquitinated proteins after cholesterol loading in our experiments can be understood as a result of attenuated autophagic flux as well, as it conforms with a previous study which demonstrated that liver-specific *Atg7* knock-out mice display liver dysfunction with intracellular accumulation of ubiquitinated protein aggregates (Komatsu *et al.*, 2005). Our study lacks analysis of protein markers that can serve to indicate autophagy induction, such as conjugation product of cleaved Atg5 with Atg12. Atg12-Atg5 forms a complex with Atg16L1 that is essential for autophagosome formation. Thus, in our study, only limited interpretation was made to determine whether cholesterol induced autophgosome formation. The level of autophagosome synthesis can be inferred by subtracting normalized LC3-II levels in the absence of cholesterol from the corresponding levels obtained in the presence of cholesterol, under CQ treatment (**Fig. 3**). This result indicates that cholesterol treatment induced small amount of autophagosome formation. Further detection of autophagy markers would be needed for more accurate interpretation.

In MTT assays, we observed that there were no additive reduction of cell viability when cells were treated with cholesterol and chloroquine at the same time. This finding implies that cholesterol *per se* has inhibited comparable degradation of autophagosomes to chloroquine. Also, it can be inferred that blockage of autophagic flux by chloroquine

treatment alone, without any disturbances in cellular homeostatic state, has only minor impacts on cell death. Although pharmacological or genetical inhibition of autophagy is enough to activate apoptosis (Boya *et al.*, 2005), our finding indicates that autophagy is important in cell survival in that it mitigates cytotoxicity when cellular homeostasis is disturbed, in this case cholesterol accumulation.

Yet, the mechanism of blunt autophagic activity under cholesterol loading remains unclear. Decreases in autophagic pathway proteins have been reported after lipid stress (Liu *et al.*, 2009; Yang *et al.*, 2010). Other mechanisms reported include reduced levels of cellular ATP (Las *et al.*, 2011), lysosomal membrane permeabilization and reduced levels of lysosomal enzymes (Inami *et al.*, 2011). One study reported that altered cholesterol level of autophagosomes and lysosomal membrane results in defects in the process of autophagosome-lysosome fusion, emphasizing the effects of changes in lipid metabolism and intracellular lipid content on autophagy (Koga *et al.*, 2010). Cholesterol is well known to pack tightly between saturated fatty acyl groups of membrane phospholipids, decreasing membrane fluidity (Ioannou, 2016). Meanwhile, excess cholesterol distributes to mitochondria, plasma membrane and ER in livers from diabetes and metabolic syndrome-related experimental NASH and in LDL-incubated primary hepatocytes (Gan *et al.*, 2014). Therefore, considering that the origin of autophagosome membrane is the preexisting cellular membrane (Carlsson and Simonsen, 2015), altered membrane cholesterol content seems to be the most prominent explanation for the reduced autophagic clearance. The fact that lipid droplet size and fusion between droplets are affected by the FC contained in phospholipid monolayer membrane of lipid droplets (Thiam *et al.*, 2013), further supports a possible direct regulatory effect of cholesterol on fusogenic capabilities. At this time, although the underlying mechanism

of lowered autophagic flux may be multifactorial, the important implication here is that dysfunction of the autophagy pathway has been linked to a variety of diseases. For instance, harmful cycle may exist in which independent factors promote both impaired autophagy and hepatic steatosis. The decrease in autophagy may aggravate steatosis, which would further impair autophagy. This cycle would worsen both cellular autophagic function and lipid accumulation perpetually (Czaja *et al.*, 2013). Critical function for autophagy in lipid metabolism is already well-established. Previous study investigated consequences of a genetic blockage of autophagy by *siATG5* on intracellular lipid content. When cells were incubated with oleate under autophagy inhibition, the level of TG significantly increased. Moreover, when cholesterol was further added, the level of intracellular cholesterol also showed significant increase compared to cells bearing normal autophagy function (Singh *et al.*, 2009).

The cholesterol in membranes affects the function of many transmembrane proteins. In particular, increased mitochondrial FC reduces mitochondrial membrane fluidity and impairs the function of mitochondrial GSH transporter, thereby promoting mitochondrial ROS generation, lipid peroxidation, and finally resulting in hepatocyte necrosis and apoptosis (Ioannou, 2016). NAD(P)H oxidase is another protein reported to be affected by membrane lipid raft. Given the fact that cholesterol accumulation in the plasma membrane promotes formation of membrane lipid raft (Gaus *et al.*, 2003) and lipid rafts are implicated in aggregation and activation of NAD(P)H oxidase (Zhang *et al.*, 2006), it is possible that cholesterol loading activates NAD(P)H oxidase and generates ROS. In the present study, increased production of intracellular ROS confirmed by DCF fluorescence images and increased level of lipid peroxides. Consistently, inhibition of autophagy by 3-methyladenine exacerbated death of cells exposed to 4-hydroxynonenal,

a lipid peroxidation product in vascular smooth muscle cells (Hill *et al.*, 2008). In animal model of autophagy disruption, isolated mitochondria from *Atg7*-deficient skeletal muscle and pancreatic beta cells exhibited a significant mitochondrial dysfunction and oxidative stress, which resulted in the physiological impairment in glucose metabolism (Wu *et al.*, 2009). Furthermore, a previous study reported that FC loading, but not free fatty acid or triglyceride loading, increased susceptibility to tumor necrosis factor-induced hepatotoxicity by depleting mitochondrial GSH (Mari *et al.*, 2006). Therefore, these results suggest that mitochondrial FC may induce NAFLD by disturbing the mitochondrial antioxidant system, which is required for hepatocytes to resist oxidative stress induced cell death. Previous studies have identified that JNK overactivation is an underlying mechanism of hepatocyte death from oxidant stress (Wang *et al.*, 2004; Wang *et al.*, 2010). Consistently, we observed an increase in phosphorylated form of JNK by cholesterol, suggesting that overactivation of the JNK may play a pivotal role in hepatocyte death from cholesterol-induced oxidative stress.

Autophagy is essential for maintaining cellular homeostasis by removing aggregated and misfolded-protein and damaged cellular organelles, such as mitochondria and ER (Mortensen *et al.*, 2010; Yang *et al.*, 2010). Therefore, accumulation of damaged organelles under defective autophagy may have further exacerbated toxic effects. We observed an increase in phosphorylated AMPK proteins and cleaved caspase-9 proteins which implies ATP depletion and mitochondrial damage.

In conclusion, the present study showed that cholesterol accumulation leads to decreases in autophagic flux and increases in oxidative stress in HepG2 cells. Reduced autophagic activity seems to aggravate oxidative stress due to attenuated removal of dysfunctional mitochondria. Cholesterol also activates JNK signaling pathway that may

have induced ATP depletion and caspase cleavage. Thus, disturbed autophagy induced by cholesterol overloading may have sensitized cells to apoptotic death from mitochondrial damage due to oxidative stress. The present study showed that cholesterol, besides free fatty acids, may contribute to lipotoxicity leading to NAFLD development.

Ⅵ. References

Arguello G, Balboa E, Arrese M and Zanlungo S (2015) Recent insights on the role of cholesterol in non-alcoholic fatty liver disease. *Biochim Biophys Acta* **1852**(9): 1765-1778.

Boya P, Gonzalez-Polo RA, Casares N, Perfettini JL, Dessen P, Larochette N, Metivier D, Meley D, Souquere S, Yoshimori T, Pierron G, Codogno P and Kroemer G (2005) Inhibition of macroautophagy triggers apoptosis. *Mol Cell Biol* **25**(3): 1025-1040.

Brookheart RT, Michel CI and Schaffer JE (2009) As a matter of fat. *Cell Metab* **10**(1): 9-12.

Byrne CD, Olufadi R, Bruce KD, Cagampang FR and Ahmed MH (2009) Metabolic disturbances in non-alcoholic fatty liver disease. *Clin Sci (Lond)* **116**(7): 539-564.

Caballero F, Fernandez A, De Lacy AM, Fernandez-Checa JC, Caballeria J and Garcia-Ruiz C (2009) Enhanced free cholesterol, SREBP-2 and StAR expression in human NASH. *J Hepatol* **50**(4): 789-796.

Carlsson SR and Simonsen A (2015) Membrane dynamics in autophagosome biogenesis. *J Cell Sci* **128**(2): 193-205.

Carrasco-Pozo C, Gotteland M, Castillo RL and Chen C (2015) 3,4-Dihydroxyphenylacetic acid, a microbiota-derived metabolite of quercetin, protects against pancreatic beta-cells dysfunction induced by high cholesterol. *Exp Cell Res* **334**(2): 270-282.

Cecconi F and Levine B (2008) The role of autophagy in mammalian development: cell makeover rather than cell death. *Dev Cell* **15**(3): 344-357.

Christian AE, Haynes MP, Phillips MC and Rothblat GH (1997) Use of cyclodextrins for manipulating cellular cholesterol content. *J Lipid Res* **38**(11): 2264-2272.

Cryns VL, Bergeron L, Zhu H, Li H and Yuan J (1996) Specific cleavage of alpha-fodrin during Fas- and tumor necrosis factor-induced apoptosis is mediated by an interleukin-1beta-converting enzyme/Ced-3 protease distinct from the poly(ADP-ribose) polymerase protease. *J Biol Chem* **271**(49): 31277-31282.

Czaja MJ, Ding WX, Donohue TM, Jr., Friedman SL, Kim JS, Komatsu M, Lemasters JJ, Lemoine A, Lin JD, Ou JH, Perlmutter DH, Randall G, Ray RB, Tsung A and Yin XM (2013) Functions of autophagy in normal and diseased liver. *Autophagy* **9**(8): 1131-1158.

Deretic V, Saitoh T and Akira S (2013) Autophagy in infection, inflammation and immunity. *Nat Rev Immunol* **13**(10): 722-737.

Fukuo Y, Yamashina S, Sonoue H, Arakawa A, Nakadera E, Aoyama T, Uchiyama A, Kon K, Ikejima K and Watanabe S (2014) Abnormality of autophagic function and cathepsin expression in the liver from patients with non-alcoholic fatty liver disease. *Hepatol Res* **44**(9): 1026-1036.

Gan LT, Van Rooyen DM, Koina ME, McCuskey RS, Teoh NC and Farrell GC (2014) Hepatocyte free cholesterol lipotoxicity results from JNK1-mediated mitochondrial injury and is HMGB1 and TLR4-dependent. *J Hepatol* **61**(6): 1376-1384.

Garbarino J, Pan M, Chin HF, Lund FW, Maxfield FR and Breslow JL (2012) STARD4 knockdown in HepG2 cells disrupts cholesterol trafficking associated with the plasma membrane, ER, and ERC. *J Lipid Res* **53**(12): 2716-2725.

Gaus K, Gratton E, Kable EP, Jones AS, Gelissen I, Kritharides L and Jessup W (2003) Visualizing lipid structure and raft domains in living cells with two-photon microscopy. *Proc Natl Acad Sci U S A* **100**(26): 15554-15559.

Hao M, Head WS, Gunawardana SC, Hasty AH and Piston DW (2007) Direct effect of cholesterol on insulin secretion: a novel mechanism for pancreatic beta-cell dysfunction. *Diabetes* **56**(9): 2328-2338.

Hill BG, Haberzettl P, Ahmed Y, Srivastava S and Bhatnagar A (2008) Unsaturated lipid peroxidation-derived aldehydes activate autophagy in vascular smooth-muscle cells. *Biochem J* **410**(3): 525-534.

Inami Y, Yamashina S, Izumi K, Ueno T, Tanida I, Ikejima K and Watanabe S (2011) Hepatic steatosis inhibits autophagic proteolysis via impairment of autophagosomal acidification and cathepsin expression. *Biochem Biophys Res Commun* **412**(4): 618-625.

Ioannou GN (2016) The Role of Cholesterol in the Pathogenesis of NASH. *Trends Endocrinol Metab* **27**(2): 84-95.

Javitt NB (1990) Hep G2 cells as a resource for metabolic studies: lipoprotein, cholesterol, and bile acids. *FASEB J* **4**(2): 161-168.

Kaur J and Debnath J (2015) Autophagy at the crossroads of catabolism and anabolism. *Nat Rev Mol Cell Biol* **16**(8): 461-472.

Kedi X, Ming Y, Yongping W, Yi Y and Xiaoxiang Z (2009) Free cholesterol overloading induced smooth muscle cells death and activated both ER- and mitochondrial-dependent death pathway. *Atherosclerosis* **207**(1): 123-130.

Koga H, Kaushik S and Cuervo AM (2010) Altered lipid content inhibits autophagic vesicular fusion. *FASEB J* **24**(8): 3052-3065.

Komatsu M, Waguri S, Ueno T, Iwata J, Murata S, Tanida I, Ezaki J, Mizushima N, Ohsumi Y and Uchiyama Y (2005) Impairment of starvation-induced and constitutive autophagy

in Atg7-deficient mice. *J Cell Biol* **169**(3): 425-434.

Korolchuk VI, Mansilla A, Menzies FM and Rubinsztein DC (2009) Autophagy inhibition compromises degradation of ubiquitin-proteasome pathway substrates. *Mol Cell* **33**(4): 517-527.

Las G, Serada SB, Wikstrom JD, Twig G and Shirihai OS (2011) Fatty acids suppress autophagic turnover in beta-cells. *J Biol Chem* **286**(49): 42534-42544.

Lee AK, Yeung-Yam-Wah V, Tse FW and Tse A (2011) Cholesterol elevation impairs glucose-stimulated Ca(2+) signaling in mouse pancreatic beta-cells. *Endocrinology* **152**(9): 3351-3361.

Liu HY, Han J, Cao SY, Hong T, Zhuo D, Shi J, Liu Z and Cao W (2009) Hepatic autophagy is suppressed in the presence of insulin resistance and hyperinsulinemia: inhibition of FoxO1-dependent expression of key autophagy genes by insulin. *J Biol Chem* **284**(45): 31484-31492.

Longatti A and Tooze SA (2009) Vesicular trafficking and autophagosome formation. *Cell Death Differ* **16**(7): 956-965.

Mari M, Caballero F, Colell A, Morales A, Caballeria J, Fernandez A, Enrich C, Fernandez-Checa JC and Garcia-Ruiz C (2006) Mitochondrial free cholesterol loading sensitizes to TNF- and Fas-mediated steatohepatitis. *Cell Metab* **4**(3): 185-198.

Martin SJ, O'Brien GA, Nishioka WK, McGahon AJ, Mahboubi A, Saido TC and Green DR (1995) Proteolysis of fodrin (non-erythroid spectrin) during apoptosis. *J Biol Chem* **270**(12): 6425-6428.

Mesmin B, Antonny B and Drin G (2013) Insights into the mechanisms of sterol transport between organelles. *Cell Mol Life Sci* **70**(18): 3405-3421.

Min HK, Kapoor A, Fuchs M, Mirshahi F, Zhou H, Maher J, Kellum J, Warnick R, Contos MJ and Sanyal AJ (2012) Increased hepatic synthesis and dysregulation of cholesterol metabolism is associated with the severity of nonalcoholic fatty liver disease. *Cell Metab* **15**(5): 665-674.

Mizushima N, Yoshimori T and Levine B (2010) Methods in mammalian autophagy research. *Cell* **140**(3): 313-326.

Molowa DT and Cimis GM (1989) Co-ordinate regulation of low-density-lipoprotein receptor and 3-hydroxy-3-methylglutaryl-CoA reductase and synthase gene expression in HepG2 cells. *Biochem J* **260**(3): 731-736.

Mortensen M, Ferguson DJ, Edelmann M, Kessler B, Morten KJ, Komatsu M and Simon AK (2010) Loss of autophagy in erythroid cells leads to defective removal of mitochondria and severe anemia in vivo. *Proc Natl Acad Sci U S A* **107**(2): 832-837.

Moscat J and Diaz-Meco MT (2009) p62 at the crossroads of autophagy, apoptosis, and cancer. *Cell* **137**(6): 1001-1004.

Nakaso K, Yoshimoto Y, Nakano T, Takeshima T, Fukuhara Y, Yasui K, Araga S, Yanagawa T, Ishii T and Nakashima K (2004) Transcriptional activation of p62/A170/ZIP during the formation of the aggregates: possible mechanisms and the role in Lewy body formation in Parkinson's disease. *Brain Res* **1012**(1-2): 42-51.

Ohkawa H, Ohishi N and Yagi K (1979) Assay for lipid peroxides in animal tissues by thiobarbituric acid reaction. *Anal Biochem* **95**(2): 351-358.

Park H-W, Park H, Semple IA, Jang I, Ro S-H, Kim M, Cazares VA, Stuenkel EL, Kim J-J, Kim JS and Lee JH (2014) Pharmacological correction of obesity-induced autophagy arrest using calcium channel blockers. *Nat Commun* **5**.

Puri P, Baillie RA, Wiest MM, Mirshahi F, Choudhury J, Cheung O, Sargeant C, Contos MJ and Sanyal AJ (2007) A lipidomic analysis of nonalcoholic fatty liver disease. *Hepatology* **46**(4): 1081-1090.

Rios-Marco P, Rios A, Jimenez-Lopez JM, Carrasco MP and Marco C (2015) Cholesterol homeostasis and autophagic flux in perifosine-treated human hepatoblastoma HepG2 and glioblastoma U-87 MG cell lines. *Biochem Pharmacol* **96**(1): 10-19.

Rong JX, Shapiro M, Trogan E and Fisher EA (2003) Transdifferentiation of mouse aortic smooth muscle cells to a macrophage-like state after cholesterol loading. *Proc Natl Acad Sci U S A* **100**(23): 13531-13536.

Rubinsztein DC, Cuervo AM, Ravikumar B, Sarkar S, Korolchuk V, Kaushik S and Klionsky DJ (2009) In search of an "autophagomometer". *Autophagy* **5**(5): 585-589.

Simonen P, Kotronen A, Hallikainen M, Sevastianova K, Makkonen J, Hakkarainen A, Lundbom N, Miettinen TA, Gylling H and Yki-Jarvinen H (2011) Cholesterol synthesis is increased and absorption decreased in non-alcoholic fatty liver disease independent of obesity. *J Hepatol* **54**(1): 153-159.

Singh R, Kaushik S, Wang Y, Xiang Y, Novak I, Komatsu M, Tanaka K, Cuervo AM and Czaja MJ (2009) Autophagy regulates lipid metabolism. *Nature* **458**(7242): 1131-1135.

Tait SWG and Green DR (2010) Mitochondria and cell death: outer membrane permeabilization and beyond. *Nat Rev Mol Cell Biol* **11**(9): 621-632.

Thiam AR, Farese Jr RV and Walther TC (2013) The biophysics and cell biology of lipid droplets. *Nat Rev Mol Cell Biol* **14**(12): 775-786.

Van Rooyen DM, Larter CZ, Haigh WG, Yeh MM, Ioannou G, Kuver R, Lee SP, Teoh NC and Farrell GC (2011) Hepatic free cholesterol accumulates in obese, diabetic mice and causes nonalcoholic steatohepatitis. *Gastroenterology* **141**(4): 1393-1403, 1403 e1391-

1395.

Vengrenyuk Y, Nishi H, Long X, Ouimet M, Savji N, Martinez FO, Cassella CP, Moore KJ, Ramsey SA, Miano JM and Fisher EA (2015) Cholesterol Loading Reprograms the MicroRNA-143/145-Myocardin Axis to Convert Aortic Smooth Muscle Cells to a Dysfunctional Macrophage-Like Phenotype. *Arterioscler Thromb Vasc Biol* **35**(3): 535-546.

Wang S, Robinet P, Smith JD and Gulshan K (2015) ORMDL orosomucoid-like proteins are degraded by free-cholesterol-loading-induced autophagy. *Proc Natl Acad Sci U S A*.

Wang Y, Schattenberg JM, Rigoli RM, Storz P and Czaja MJ (2004) Hepatocyte resistance to oxidative stress is dependent on protein kinase C-mediated down-regulation of c-Jun/AP-1. *J Biol Chem* **279**(30): 31089-31097.

Wang Y, Singh R, Xiang Y and Czaja MJ (2010) Macroautophagy and chaperone-mediated autophagy are required for hepatocyte resistance to oxidant stress. *Hepatology* **52**(1): 266-277.

Wouters K, van Gorp PJ, Bieghs V, Gijbels MJ, Duimel H, Lutjohann D, Kerksiek A, van Kruchten R, Maeda N, Staels B, van Bilsen M, Shiri-Sverdlov R and Hofker MH (2008) Dietary cholesterol, rather than liver steatosis, leads to hepatic inflammation in hyperlipidemic mouse models of nonalcoholic steatohepatitis. *Hepatology* **48**(2): 474-486.

Wu JJ, Quijano C, Chen E, Liu H, Cao L, Fergusson MM, Rovira, II, Gutkind S, Daniels MP, Komatsu M and Finkel T (2009) Mitochondrial dysfunction and oxidative stress mediate the physiological impairment induced by the disruption of autophagy. *Aging (Albany NY)* **1**(4): 425-437.

Xu K, Yang Y, Yan M, Zhan J, Fu X and Zheng X (2010) Autophagy plays a protective role in free cholesterol overload-induced death of smooth muscle cells. *J Lipid Res* **51**(9): 2581-2590.

Yang L, Li P, Fu S, Calay ES and Hotamisligil GS (2010) Defective hepatic autophagy in obesity promotes ER stress and causes insulin resistance. *Cell Metab* **11**(6): 467-478.

Yao PM and Tabas I (2001) Free cholesterol loading of macrophages is associated with widespread mitochondrial dysfunction and activation of the mitochondrial apoptosis pathway. *J Biol Chem* **276**(45): 42468-42476.

Yu C, Huang X, Xu Y, Li H, Su J, Zhong J, Kang J, Liu Y and Sun L (2013) Lysosome dysfunction enhances oxidative stress-induced apoptosis through ubiquitinated protein accumulation in Hela cells. *Anat Rec (Hoboken)* **296**(1): 31-39.

Zhang AY, Yi F, Zhang G, Gulbins E and Li P-L (2006) Lipid raft clustering and redox signaling platform formation in coronary arterial endothelial cells. *Hypertension* **47**(1): 74-80.

Zhang X-j, Chen S, Huang K-x and Le W-d (2013) Why should autophagic flux be assessed? *Acta Pharmacol Sin* **34**(5): 595-599.

Zhao YF, Wang L, Lee S, Sun Q, Tuo Y, Wang Y, Pei J and Chen C (2010) Cholesterol induces mitochondrial dysfunction and apoptosis in mouse pancreatic beta-cell line MIN6 cells. *Endocrine* **37**(1): 76-82.

Zidovetzki R and Levitan I (2007) Use of cyclodextrins to manipulate plasma membrane cholesterol content: evidence, misconceptions and control strategies. *Biochim Biophys Acta* **1768**(6): 1311-1324.

국문 초록

HepG2 세포주에서 콜레스테롤에 의한 자가포식과 세포 사멸 연구

서울대학교 대학원 식품영양학과

김소라

비알콜성 지방간질환(NAFLD)은 전세계적으로 비만과 제2형 당뇨병이 증가하면서 그 유병률이 크게 증가하고 있으며 바이러스, 알코올, 약물, 유전에 의한 간질환을 제외하고, 원인을 모르는 간질환의 90%를 차지하는 가장 흔한 만성 질환이다. 최근 다수의 연구에서 이 비알콜성 지방간질환의 발병 시 간에 과다한 콜레스테롤이 축적됨을 보고하고 있으므로 콜레스테롤은 간에 독성을 일으키는 지질대사물로 주목 받고 있다. 자가포식은 세포의 방어기전으로 세포에 가해지는 스트레스 상황에서 대사물질을 제공하는 적응 반응인 동시에 유해 물질 및 단백질, 지질, 소기관을 포함한 물질들을 분해하여 항상성을 유지하는 기전이다. 이러한 맥락에서 본 연구는 간세포에 과다하게 축적된 콜레스테롤이 세포 독성을 일으키는지 확인하고자 하였으며 세포 내 콜레스테롤 항상성이 깨진 스트레스 상황에서 자가포식의 활성에 변화가 생기는지, 또 변화된 자가포식 기전이 콜레스테롤에 의한 세포 독성에 기여하는 지 확인하고자

하였다. 간세포에 축적된 콜레스테롤의 독성과 이 스트레스 환경에서 자가포식 기전의 역할을 살펴보기 위하여 인간 간암 세포주인 HepG2 세포주가 배양되는 배지에 25 혹은 50 μg/mL 농도의 콜레스테롤을 녹여 처리하였다. 사용된 콜레스테롤의 농도는 비알콜성 지방간염 환자의 간이나 실험 동물의 간에서 확인된 콜레스테롤 축적 양과 비슷한 세포 내 축적을 일으켰다. 콜레스테롤을 24시간 처리하자 세포 내 총콜레스테롤의 양이 50 μg/mL 농도의 콜레스테롤 처리 시 대조군에 비해 유의적으로 증가하였다. MTT assay, 현미경 관찰을 통해 콜레스테롤 처리 시 세포 생존율이 감소하는 것을 확인하였으며 Western blotting을 통한 spectrin 단백질과 caspase-3 단백질의 분해 검출을 통해 HepG2 세포에서 자연 사멸이 발생함을 확인하였다. 한편, 자가포식과 관련된 단백질을 측정한 결과 콜레스테롤의 처리는 LC3-II, p62 단백질의 유의적인 증가를 일으켰으며 Beclin-1 단백질은 차이가 없었다. 또한, 라이소좀 저해제인 chloroquine을 함께 처리하여 관찰한 결과 자가포식 유동양(autophagic flux)이 콜레스테롤을 처리하지 않았을 경우에 비해 현저하게 감소함을 확인하였고, 동시에 자가포식의 분해물로 지정된 ubiquitinated protein의 축적이 일어남을 확인하였다. 자가포식의 저해는 caspase-3 활성을 일으켜 세포 자연 사멸을 초래한다고 알려져 있으므로 자가포식의 저해가 콜레스테롤에 의한 세포 독성의 주요 기전인지 확인하기 위해 chloroquine과 콜레스테롤을 처리하여 MTT assay를 통해 세포 활성을 시험하였다. 그 결과 50 μg/mL 농도의 콜레스테롤과 10 μM 농도의 chloroquine 처리의 자가포식 저해 정도가 비슷한 수준인 것과 달리 chloroquine의 단독 처리는 경미한 세포 활성 저해만을 나타내어 자가포식 이외에 세포 사멸을 초래하는 콜레스테롤의 독성 기전이 있음을 확인하였다. 실험 결과, 50

μg/mL 농도의 콜레스테롤의 처리가 세포 내 활성 산소와 지질 과산화물의 증가로 대변되는 산화스트레스 지표의 유의적인 변화를 일으킴을 확인했다. 또한, 산화스트레스와 관련하여 JNK 단백질의 인산화 증가를 관찰하였고, 이와 연관이 깊은 비정상적인 미토콘드리아의 지표로서 cleaved caspase-9 단백질 수준의 증가를 확인하였으며, ATP 고갈의 간접적인 증거로서 AMPK 인산화형의 증가를 확인하였다. 결론적으로, 본 실험에서 과다한 간의 콜레스테롤 축적은 자가포식 유동성을 감소시키고 산화스트레스 및 미토콘드리아 이상을 일으켜 세포 자연 사멸을 촉진함을 확인하였다. 비록 감소한 자가포식 활성 그 자체가 전적으로 간세포 사멸을 일으키진 않았지만, 비정상적인 미토콘드리아 제거를 저해시켜 산화 스트레스로 표현되는 세포 독성을 증가시켰을 가능성이 있다. 전체적으로 본 연구는 기존에 비알콜성 간질환에서 독성 물질로 연구된 유리 지방산 이외에 콜레스테롤 역시 간 세포에 직접적으로 독성을 일으킬 수 있음을 확인하였고, 비알콜성 간질환에서 나타나는 자가 포식 저해 현상에 콜레스테롤이 기여할 수 있음을 처음으로 확인한 데에 의의가 있다.

주요어: 간세포, 미토콘드리아, 산화스트레스, 세포사멸, 자가포식, 콜레스테롤

학번: 2014-205275